9.3 Exercises

9.1 Construct SATURNE I (weak index) synchrotron. Spin Resonances
Solution: page 315.

In this exercise, the weak focusing 3 GeV synchrotron SATURNE I is modeled. Spin resonances in a weak dipole gradient lattice are observed.

Table 9.1 Parameters of SATURNE I weak focusing synchrotron [25]. ρ_0 denotes the reference bending radius in the dipole; the reference orbit, field index, wave numbers, etc., are taken along that radius

Orbit length, C	cm	6890
Average radius, $R = C/2\pi$	cm	1096.58
Drift length, $2l$	cm	400
Magnetic radius, ρ_0	cm	841.93
$R/\rho_0 = 1 + k$		1.30246
Field index n, nominal		0.6
Wave numbers ν_x, ν_y, nominal		0.72, 0.89
Stability limit		$0.5 < n < 0.757$
Injection energy (proton)	MeV	3.6
Field at injection	kG	0.326
Top energy	GeV	2.94
Field at top energy, B_{max}	kG	14.9
$\dot{B}$	kG/s	18
Synchronous energy gain	keV/turn	1.160
RF harmonic		2

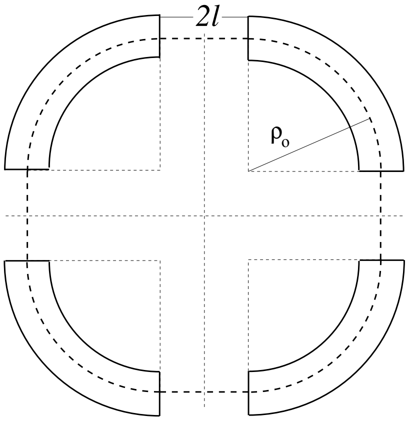

Fig. 9.22 A schematic layout of SATURNE I, a $2\pi/4$ axial symmetry structure, comprised of 4 radial field index 90 deg dipoles and 4 drift spaces. The cell in the simulation exercises is taken as a $\pi/2$ quadrant: half-drift / 90^o-dipole / half-drift

(a) Construct a model of SATURNE I 90^o cell dipole in the hard-edge model, using DIPOLE. Use the parameters given in Tab. 9.1, and Fig. 9.22 as a guidance. For beam monitoring purposes, split the dipole in two 45^odeg halves. It is judicious to take RM=841.93 cm in DIPOLE, as this is the reference radius for the definition of the radial index. Take an integration step size in centimeter range - small enough to ensure numerical convergence, as large as doable for fast multiturn raytracing.

Validate the model by producing the 6×6 transport matrix of the cell dipole (MATRIX[IFOC=0] can be used for that, with OBJET[KOBJ=5] to define a proper set of paraxial initial coordinates) and checking against theory (Sect. 15.2, Eq. 15.6).

(b) Construct a model of SATURNE I cell, with origin at the center of the drift. Find the closed orbit, that particular trajectory which has all its coordinates zero in the drifts: use DIPOLE[KPOS] to cancel the closed orbit coordinates at DIPOLE ends. While there, check the expected value of the dispersion (Eq. 9.26) and of the momentum compaction (Eq. 9.28), from the raytracing of a chromatic closed orbit - *i.e.*, the orbit of an off-momentum particle. Plot these two orbits (on- and off-momentum), over a complete turn around the ring, on a common graph.

Compute the cell periodic optical functions and tunes, using either MATRIX[IFOC=11] or TWISS; check their values against theory. Check consistency with previous dispersion function and momentum compaction outcomes.

Move the origin of the lattice at a different azimuth s along the cell: verify that, while the transport matrix depends on the origin, its trace does not.

Produce a graph of the optical functions (betatron functions and dispersion) along the cell. Check the expected average values of the betatron functions (Eq. 9.20).

Produce a scan of the tunes over the field index range $0.5 \le n \le 0.757$. REBELOTE can be used to repeatedly change n over that range. Superimpose the theoretical curves $\nu_x(n)$, $\nu_y(n)$.

(c) Justify considering the betatron oscillation as sinusoidal, namely,

$$y(\theta) = A\,\cos(\nu_y\theta + \phi)$$

wherein $\theta = s/R$, $R = \oint ds/2\pi$.

(d) Launch a few particles evenly distributed on a common paraxial horizontal Courant-Snyder invariant, vertical motion taken null (OBJET[KOBJ=8] can be used), for a single pass through the cell. Store particle data along the cell in zgoubi.plt, using DIPOLE[IL=2] and DRIFT[split,N=20,IL=2]. Use these to generate a graph of the beam envelopes.

Using Eq. 9.22 compare with the results obtained in (b). Find the minimum and maximum values of the betatron functions, and their azimuth $s(min[\beta_x])$, $s(max[\beta_x])$. Check the latter against theory.

Repeat for the vertical motion, taking $\varepsilon_x = 0$, ε_y paraxial.

Repeat, using, instead of several particles on a common invariant, a single particle traced over a few tens of turns.

(e) Produce an acceleration cycle from 3.6 MeV to 3 GeV, for a few particles launched on a common $10^{-4}\,\pi$m initial invariant in each plane. Ignore synchrotron motion (CAVITE[IOPT=3] can be used in that case). Take a peak voltage $\hat{V} = 200$ kV (unrealistic though, as it would result in a nonphysical $\dot{B}$ (Eq. 9.29)) and synchronous phase $\phi_s = 150$ deg (justify $\phi_s > \pi/2$).

Check the betatron damping over the acceleration range: compare with theory (Eq. 9.31).

How close to symplectic the numerical integration is (it is by definition *not* symplectic, being a truncated Taylor series method [26, Eq. 1.2.4]), depends on the integration step size, and on the size of the flying mesh in the DIPOLE method [26, Fig. 20]; check a possible departure of the betatron damping from theory as a function of these parameters.

Produce a graph of the horizontal and vertical wave number values over the acceleration cycle.

(f) Some spin motion, now. Adding SPNTRK at the beginning of the sequence used in (e) will ensure spin tracking.

Based on the input data file worked out for question (d), simulate the acceleration of a single particle, through the intrinsic resonance $G\gamma_R = 4 - \nu_y$, from a distance of a few times the resonance strength upstream (this requires determining BORO value under OBJET) to a distance of a few times the resonance strength downstream of the resonance, at an acceleration rate of 10 kV/turn.

OBJET[KOBJ=8] can be used to allow to easily define an initial invariant value.

Start with spin vertical. On a common graph, plot $S_y(turn)$ for a few different values of the vertical betatron invariant (the horizontal invariant value does not matter - explain that statement, it can be taken zero). Derive the resonance strength from these tracking, check against theory.

Repeat, for different crossing speeds.

Push the tracking beyond $G\gamma = 2{\times}4{+}\nu_y$: verify that the sole systematic resonances $G\gamma = \text{integer} \times P \pm \nu_y$ are excited - with $P = 4$ the periodicity of the ring.

Break the 4-periodicity of the lattice by perturbing the index in one of the 4 dipoles (say, by 10%), verify that all resonances $G\gamma = \text{integer} \pm \nu_y$ are now excited.

(g) Consider a case of weak resonance crossing, single particle (*i.e.*, a case where $P_f/P_i \approx 1$, taken from (f); crossing speed may be increased, or particle invariant decreased if needed), show that it satisfies Eq. 9.41. Match its turn-by-turn tracking data to Eq. 9.41 so to get the vertical betatron tune ν_y, the location of the resonance $G\gamma_\mathrm{R}$, and its strength.

(h) Stationary spin motion (*i.e.* at fixed energy) is considered in this question. Track a few particles with distances from the resonance $\Delta = G\gamma - G\gamma_R = G\gamma - (4 - \nu_y)$ evenly spanning the interval $\Delta \in [0, 7 \times \epsilon_R]$.

Produce on a common graph the spin motion $S_y(turn)$ for these particles, as observed at some azimuth along the ring.

Produce a graph of $\langle S_y \rangle|_\mathrm{turn}(\Delta)$ (as in Fig. 9.19). Produce the vertical betatron tune ν_y, the location of the resonance $G\gamma_\mathrm{R}$, and its strength, obtained from a match of $\langle S_y \rangle|_\mathrm{turn}(\Delta)$ to (Eq. 9.37)

$$\langle S_y \rangle (\Delta) = \frac{\Delta}{\sqrt{|\epsilon_R|^2 + \Delta^2}}$$

(i) Track a 200-particle 6-D bunch, with Gaussian transverse densities of $\varepsilon_\mathrm{x,y}$ a few μm, and Gaussian $\delta p/p$ with $\sigma_{\delta p/p} = 10^{-4}$. Produce a graph of the average value of S_y over a 200 particle set, as a function of $G\gamma$, across the $G\gamma_R = 4 - \nu_y$ resonance. Indicate on that graph the location of the resonant $G\gamma_R$ values.

Perform this resonance crossing for five different values of the particle invariant: $\varepsilon_y/\pi = 2,\ 10,\ 20,\ 40,\ 200\,\mu$m. Compute P_f/P_i in each case, check the dependence on ε_y against theory.

Compute the resonance strength, ε_y, from these tracking.

Re-do this crossing simulation for a different crossing speed (take for instance $\hat{V} = 10\,$kV) and a couple of vertical invariant values, compute P_f/P_i so obtained. Check the crossing speed dependence of P_f/P_i against theory.

9.2 Construct the ZGS (zero-gradient) synchrotron. Spin Resonances

Solution: page 339.

In this exercise, the ZGS 12 GeV synchrotron is modeled. Spin resonances in a zero-gradient, wedge focusing synchrotron are studied.

A photo taken in the ZGS tunnel is given in Fig. 9.4; a schematic layout of the ring is shown in Fig. 9.23, and a sketch of the double dipole cell in Fig. 9.24. Table 9.2 details the parameters of the synchrotron resorted to in these simulations.

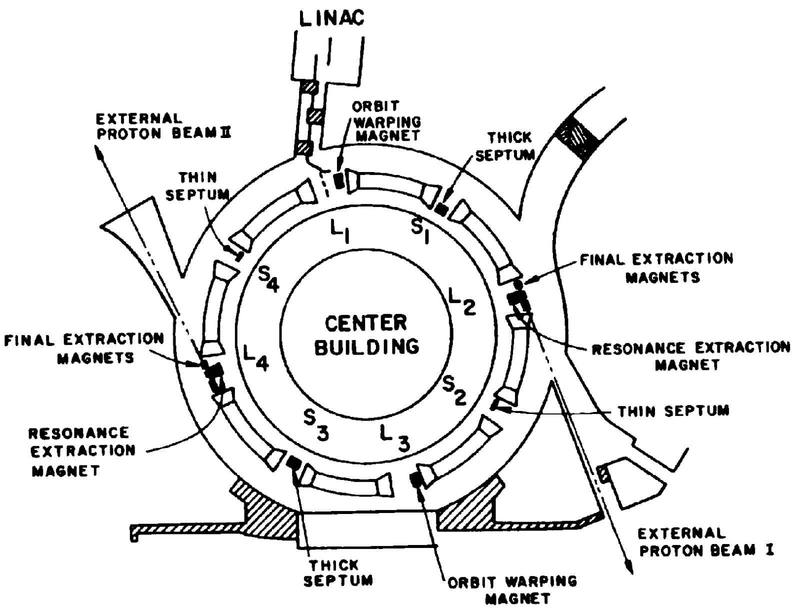

Fig. 9.23 A schematic layout of the ZGS [23], a $\pi/2$-periodic structure, comprised of 8 zero-index dipoles, 4 long and 4 short straight sections

(a) Construct a model of ZGS 45^o cell dipole in the hard-edge model, using DIPOLE. Use the parameters given in Tab. 9.2, and Figs. 9.23, 9.24 as a guidance. For beam monitoring purposes, split the dipole in two 22.5^odeg halves. Take the closed orbit radius as the reference RM=2076 cm in DIPOLE: it will be assumed that the orbit is the same at all energies[4]. Take an integration step size in centimeter range - small enough to ensure numerical convergence, as large as doable for fast multiturn raytracing.

Validate the model by producing the 6×6 transport matrices of both dipole (MATRIX[IFOC=0] can be used for that, with OBJET[KOBJ=5] to define a proper set of paraxial initial coordinates) and checking against theory (Sect. 15.2, Eq. 15.6).

Add fringe fields in DIPOLE[λ,$C_0 - C_5$], the rest if the exercise will use that model. Take fringe field extent and coefficient values

$$\lambda = 60\,\text{cm}\ C_0 = 0.1455,\ C_1 = 2.2670,\ C_2 = -0.6395,\ C_3 = 1.1558,\ C_4 = C_5 = 0 \tag{9.43}$$

($C_0 - C_5$ determine the shape of the field fall-off, they have been computed from a typical measured field profile $B(s)$).

(b) Construct a model of ZGS cell accounting for dipole fringe fields, with origin at the center of the long drift. In doing so, use DIPOLE[KPOS] to cancel the closed orbit coordinates at DIPOLE ends.

Compute the periodic optical functions at cell ends, and cell tunes, using MATRIX[IFOC=11]; check their values against theory.

Move the origin at the location (azimuth s along the cell) of the betatron functions extrema: verify that, while the transport matrix depends on the origin, its trace does not. Verify that the local betatron function extrema, and the dispersion function, have the expected values.

Produce a graph of the optical functions (betatron functions and dispersion) along the cell.

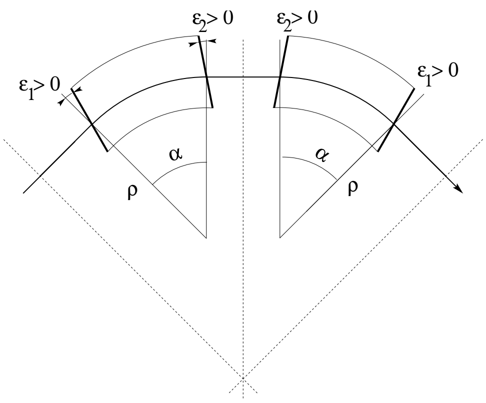

Fig. 9.24 A sketch of ZGS cell layout. In defining the entrance and exit faces (EFBs) of the magnet, beam goes from left to right. Wedge angles at the long straight sections (ε_1) and at the short straight sections (ε_2) are different

(c) Additional verifications regarding the model.

Produce a graph of the field B(s)

---

[4] Note that in reality the reference orbit in ZGS moved outward during acceleration [27].

Table 9.2 Parameters of the ZGS weak focusing synchrotron after Refs. [27, 28] [23, pp. 288-294,p. 716] (2nd column, when they are known) and in the present simplified model and numerical simulations (3rd column). Note that the actual orbit moves during ZGS acceleration cycle, tunes change as well - this is not taken into account in the present modeling, for simplicity

		From Refs. [27, 28]	**Simplified model**
Injection energy	MeV	50	
Top energy	GeV	12.5	
$G\gamma$ span		1.888387 - 25.67781	
Length of central orbit	m	171.8	170.90457
Length of straight sections, total	m	41.45	40.44
Lattice			
Wave numbers ν_x; ν_y		0.82; 0.79	0.849; 0.771
Max. β_x; β_y	m		32.5; 37.1
Magnet			
Length	m	16.3	16.30486 (magnetic)
Magnetic radius	m	21.716	20.76
Field min.; max.	kG	0.482; 21.5	0.4986; 21.54
Field index		0	
Yoke angular extent	deg	43.02590	45
Wedge angle	deg	≈10	13 and 8
RF			
Rev. frequency	MHz	0.55 - 1.75	0.551 - 1.751
RF harmonic h=$\omega_{\rm rf}/\omega_{\rm rev}$		8	
Peak voltage	kV	20	200
B-dot, nominal/max.	T/s	2.15/2.6	
Energy gain, nominal/max.	keV/turn	8.3/10	100
Synchronous phase, nominal	deg	150	
Beam			
ε_x; ε_y (at injection)	$\pi\mu$m	25; 150	
Momentum spread, rms		3×10^{-4}	
Polarization at injection	%	>75	100
Radial width of beam (90%), at inj.	inch	2.5	$\sqrt{\beta_x\varepsilon_x/\pi}=1.1$

- along the on-momentum closed orbit, and along off-momentum chromatic closed orbits, across a cell;

- along orbits at large horizontal excursion;

- along orbits at large vertical excursion.

For all these cases, verify qualitatively, from the graphs, that $B(s)$ appears as expected.

(d) Justify considering the betatron oscillation as sinusoidal, namely,

$$y(\theta) = A\ \cos(\nu_y\theta + \phi)$$

wherein $\theta = s/R$, $R = \oint ds/2\pi$.

(e) Produce an acceleration cycle from 50 MeV to 17 GeV about, for a few particles launched on a common $10^{-5}\,\pi$m vertical initial invariant, with small horizontal invariant. Ignore synchrotron motion (CAVITE[IOPT=3] can be used in that case).

Take a peak voltage $\hat{V} = 200\,\mathrm{kV}$ (this is unrealistic but yields 10 times faster computing than the actual $\hat{V} = 20\,\mathrm{kV}$, Tab. 9.2) and synchronous phase $\phi_s = 150\,\mathrm{deg}$ (justify $\phi_s > \pi/2$). Add spin, using SPNTRK, in view of the next question, (f).

Check the accuracy of the betatron damping over the acceleration range, compared to theory. How close to symplectic the numerical integration is (it is by definition *not* symplectic), depends on the integration step size, and on the size of the flying mesh in the DIPOLE method [26, Fig. 20]; check a possible departure of the betatron damping from theory as a function of these parameters.

Produce a graph of the evolution of the horizontal and vertical wave numbers during the acceleration cycle.

(f) Using the raytracing material developed in (e): produce a graph of the vertical spin component of a few particles, and the average value over the 200 particle bunch, as a function of $G\gamma$. Indicate on that graph the location of the resonant $G\gamma_R$ values.

(g) Based on the simulation file used in (f), simulate the acceleration of a single particle, through one particular intrinsic resonance, from a few thousand turns upstream to a few thousand turns downstream.

Perform this resonance crossing for different values of the particle invariant. Determine the dependence of final/initial vertical spin component value, on the invariant value; check against theory.

Re-do this crossing simulation for a different crossing speed. Check the crossing speed dependence of final/initial vertical spin component so obtained, against theory.

(h) Introduce a vertical orbit defect in the ZGS ring.

Find the closed orbit.

Accelerate a particle launched on that closed orbit, from 50 MeV to 17 GeV about, produce a graph of the vertical spin component.

Select one particular resonance, reproduce the two methods of (g) to check the location of the resonance at $G\gamma_R$ =integer, and to find its strength.

References

1. Veksler, V.: A new method of acceleration of relativistic particles. J. of Phys. USSR 9 153-158 (1945)
2. McMillan, E. M.: The Synchrotron. Phys. Rev. 68 143-144 (1945)
3. Goward, F. K., and Barnes, D. E.: Experimental 8 MeV synchrotron for electron acceleration. Nature 158, 413 (1946)
4. Richardson, J.R., et al.: Frequency Modulated Cyclotron. Phys. Rev. 69: 669 (1946)
5. Kerst, D. W.: The Acceleration of Electrons by Magnetic Induction.. Phys. Rev., 60, 47-53 (1941)
6. SATURNE I photos: FAR_SA_N_00248, FAR_SA_N_02826; credit CEA Saclay. Archives historiques CEA. Copyright CEA/Service de documentation
7. Sessler, A., Wilson, E.: Engines of Discovery. A Century of Particle Accelerators. World Scientific, 2007
8. Fig. 9.3: Credit Reider Hahn, Fermilab
9. Endo, K., et al.: Compact proton and carbon ion synchrotrons for radiation therapy. MOPRI087, Proceedings of EPAC 2002, Paris, France; pp. 2733-2735. https://accelconf.web.cern.ch/e02/PAPERS/MOPRI087.pdf
10. Vostrikov, V.A., et al.: Novel approach to design of the compact proton synchrotron magnetic lattice. tupsa17, 26th Russian Particle Accelerator Conference RUPAC2018, Protvino, Russia (2018). https://accelconf.web.cern.ch/rupac2018/papers/tupsa17.pdf
11. Cohen, D, : Feasibility of Accelerating Polarized Protons with the Argonne ZGS. Review of Scientific Instruments 33, 161 (1962).// https://doi.org/10.1063/1.1746524
12. Ratner, L.G. and Khoe, T.K.: Acceleration of Polarized Protons in the Zero Gradient Synchrotron. Procs. PAC 1973 Conference, Washington (1973). http://accelconf.web.cern.ch/p73/PDF/PAC1973_0217.PDF
13. Bywatwr, J., Khoe, T., et al.: A pulsed quadrupole system for preventing depolarization. IEEE Transactions on Nuclear Science (Volume: 20, Issue: 3, June 1973)
14. Cho, Y., et als.: Effects of depolarizing resonances on a circulating beam of polarized protons during or storage in a synchrotron. IEEE Trans. Nuclear Science, Vol.NS-24, No.3, June 1977
15. Parker, E.F.: High Energy Polarized Deuterons at the Argonne National Laboratory Zero Gradient Synchrotron. IEEE Transactions on Nuclear Science, Vol. NS-26, No. 3, June 1979, pp 3200-3202

16. Suddeth, D.E., et als.: Pole face winding equipment for eddy current correction at the Zero Gradient Synchrotron. Procs. PAC 1973 Conference, Washington (1973). http://accelconf.web.cern.ch/p73/PDF/PAC1973_0397.PDF
17. Rauchas, A.V. and Wright, A.J.: Betatron tune profile control in the Zero Gradient Synchrotron (ZGS) using the main magnet pole face windings. Procs. PAC1977 conference, IEEE Trans. on Nucl. Science, VoL.NS-24, No.3, June 1977
18. Floquet, G.: Sur les équations différentielles linéaires à coefficients périodiques. Annales scientifiques de l'E.N.S. 2e série, tome 12 (1883), p. 47-88. http://www.numdam.org/item?id=ASENS_1883_2_12__47_0
19. Leleux, G.: Accélérateurs Circulaires. Lecture Notes, INSTN, CEA Saclay (1978)
20. Leleux, G.: Traversée des résonances de dépolarisation. Rapport Interne LNS/GT-91-15, SATURNE, Groupe Théorie, CEA Saclay (février 1991)
21. Méot, F.: Spin Dynamics. In: Polarized Beam Dynamics and Instrumentation in Particle Accelerators, USPAS Summer 2021 Spin Class Lectures, Springer Nature, Open Acess (2023). https://link.springer.com/book/10.1007/978-3-031-16715-7
22. Lee, S.Y.: Spin Dynamics and Snakes in Synchrotrons. World Scientific, 1997
23. Khoe, T.K., et al.: The High Energy Polarized Beam at the ZGS. Procs. IXth Int. Conf on High Energy Accelerators, Dubna, pp. 288-294 (1974).
Fig. 9.16: Copyrights under license CC-BY-3.0, https://creativecommons.org/licenses/by/3.0; no change to the material
24. Froissart, M. and Stora, R.: Dépolarisation d'un faisceau de protons polarisés dans un synchrotron. Nucl. lnst. Meth. 7 (l960) 297.
25. Bruck H., Debraine P., Levy-Mandel R., Lutz J., Podliasky I., Prevot F., Taieb J., Winter S.D., Maillet R., Caractéristiques principales du Synchrotron à Protons de Saclay et résultats obtenus lors de la mise en route, rapport CEA no.93, CEN-Saclay, 1958.
26. Méot, F.: Zgoubi Users' Guide. https://www.osti.gov/biblio/1062013-zgoubi-users-guide Sourceforge latest version: https://sourceforge.net/p/zgoubi/code/HEAD/tree/trunk/guide/Zgoubi.pdf
27. Foss, M.H., et al.: The Argonne ZGS Magnet. IEEE 1965, pp. 377-382, June 1965
28. Klaisner, L.A., et al.: IEEE 1965, pp. 133-137, June 1965